Low-lying states in ^{20}Ne populated by the ^{19}F(^{7}Li,^{6}He)^{20}Ne reaction at 34 MeV†

M. E. Williams-Norton,* G. M. Hudson, K. W. Kemper, G. E. Moore,‡ G. A. Norton,§ R. J. Puigh, and A. F. Zeller‖

Department of Physics, The Florida State University, Tallahassee, Florida 32306

(Received 4 August 1975)

Angular distributions have been measured for transitions to ^{20}Ne states up to 7.43 MeV in excitation populated in the ^{19}F(^{7}Li, ^{6}He)^{20}Ne reaction at $E_{^{7}\mathrm{Li}}$=34 MeV. Elastic scattering of ^{6}Li and ^{7}Li at 34 MeV from ^{19}F was also performed and optical model parameters were determined from fits to the measured angular distributions. These optical model parameters were used in finite-range distorted-width Born-approximation analyses of the single nucleon transfer data to extract spectroscopic factors for states at 0.0, 1.634, 4.247, 5.785, 6.722, and 7.424 MeV excitation in ^{20}Ne. Spectroscopic factors obtained from this reaction agree well with those from light-ion transfer reactions. However, the $2s_{1/2}$ calculation for the ^{20}Ne ground state is out of phase with the data by 7°. The "j-forbidden" 4^+ state at 4.247 MeV excitation is found to be weakly excited in the ^{19}F(^{7}Li, ^{6}He)^{20}Ne reaction.

[NUCLEAR REACTIONS ^{19}F(^{6}Li, ^{6}Li), (^{7}Li, ^{7}Li), (^{7}Li, ^{6}He), E=34 and 37 MeV; measured $\sigma(\theta)$; deduced optical model parameters, deduced S for ^{20}Ne. Natural targets, finite range DWBA analysis, resolution 150 keV, θ=1–50°, $\Delta\theta$=2–2.5°.]

I. INTRODUCTION

A recent study of the ^{62}Ni(^{7}Li, ^{6}He)^{63}Cu reaction[1,2] showed that it was possible to distinguish between $2p_{3/2}$ and $2p_{1/2}$ single particle states, describe the shapes of the measured angular distributions well with the finite-range distorted-wave Born approximation (DWBA), and extract spectroscopic factors which agree well with those obtained with light-ion transfer reactions. These results indicated understanding of the (^{7}Li, ^{6}He) reaction in that mass region.

Spectroscopic information about states in ^{20}Ne has been obtained from the ^{19}F(^{3}He, d)^{20}Ne and ^{19}F(d, n)^{20}Ne reactions.[3-5] Because nuclei in the A=20 region have large deformations,[6] large collective inelastic excitations occur, and it is expected that multistep processes in single nucleon transfer reactions are important. The strong population of the "j-forbidden" 4^+ state at 4.247 MeV excitation in ^{20}Ne by the ^{19}F(^{3}He, d)^{20}Ne reaction[3] is one example of a transition where multistep processes produce a large cross section. In the present work, the ^{19}F(^{7}Li, ^{6}He)^{20}Ne reaction is studied in order to determine how well the transitions populating the low-lying states in ^{20}Ne can be described by the finite-range DWBA. Experimental data include differential cross sections for the proton transfer reaction populating states at 0.0, 1.634, 4.247, 5.785, 6.722, and 7.424 MeV excitation in ^{20}Ne and elastic scattering of 34 MeV ^{6}Li and ^{7}Li by ^{19}F. Optical model parameters extracted from fitting the elastic data were used in the finite-range DWBA analysis. Spectroscopic factors have been extracted and compared to those obtained in the light-ion transfer reactions. Reaction data at 37 MeV were taken at a few angles to determine if the transfer reaction cross section varied with energy. Preliminary results of this work were reported earlier.[7]

II. EXPERIMENTAL PROCEDURE

Beams of ^{6}Li$^-$ and ^{7}Li$^-$, produced initially by a Heinicke direct extraction negative ion source,[8] a sputter source,[9] and finally with an inverted sputter source,[10] were injected into the Florida State University Super FN tandem Van de Graaff. Beam currents on target varied from 100 to 400 nA at 34 MeV. Targets of natural CaF_2 evaporated onto 20 μg/cm^2 carbon backings were 40 to 80 μg/cm^2 thick.

Reaction data from 1° to 20° and elastic scattering data for both ^{6}Li + ^{19}F and ^{7}Li + ^{19}F, from 12.5° to 35°, were taken in 2° or 2.5° steps in the Florida State University quadrupole spectrometer.[11] A standard scattering chamber was used to take reaction data from 17.5° to 40° and elastic scattering data from 25° to 45° (in 2.5° steps). The angular resolution in the horizontal plane was 0.5° for the quadrupole data, and 0.2° for the scattering chamber data. A ΔE-E counter telescope consisting of 75 μm and 700 μm Si surface barrier detectors, respectively, was used to detect reaction

products at all angles and elastically scattered ^{6}Li and ^{7}Li at angles $\geq 25°$. The experimental energy resolution was approximately 150 keV. Elastic scattering forward of 25° was detected with a single 700 μm E detector. Resolution for the single counter was 80–100 keV. Pulse height information corresponding to coincident $\Delta E, E$ events was stored via a CAMAC interface in an EMR 6130 computer. Regions corresponding to different particle groups were drawn on a two dimensional display of ΔE vs E. The boundaries of these regions served as gates to sort events into linear energy spectra. A monitor detector was used to check for target deterioration and allow for relative normalization among data taken at different angles.

III. EXPERIMENTAL RESULTS

Elastic scattering of ^{7}Li at 20 and 34 MeV and ^{19}F(^{7}Li, ^{6}He)^{20}Ne reaction data ($E_{^7\mathrm{Li}}$ = 34 MeV) were all obtained at several angles using the same CaF_2 target. The 20 MeV ^{7}Li elastic yields on ^{40}Ca were normalized to optical model cross sections using parameters obtained by Bethge, Fou, and Zurmühle.[12] Absolute cross sections for the elastic scatterings and the (^{7}Li, ^{6}He) reaction on ^{19}F were calculated assuming the target contained two F atoms for each Ca atom and referring ^{6}He and elastic ^{7}Li and ^{6}Li yields at 34 and 37 MeV to the 20 MeV elastic scattering cross sections. The error in this normalization procedure is estimated to be about 12%. Combined statistical, background subtraction, and peak separation errors in the elastic scattering and ^{19}F(^{7}Li, ^{6}He)^{20}Ne reaction differential cross sections range from 1% for elastic scattering at forward angles to 30% for weak ^{20}Ne states at back angles. The absolute cross sections for the quadrupole spectrometer data were obtained by normalizing to data taken in the scattering chamber at 17.5° and 20°. At 34 MeV angular distributions were obtained for states at 0.0 (0^+), 1.634 (2^+), 4.247 (4^+), 5.785 (1^-), 6.722 (0^+), and 7.424 MeV (2^+) excitation in ^{20}Ne. A spectrum of ^{19}F(^{7}Li, ^{6}He)^{20}Ne at $\theta_{\mathrm{lab}} = 17.5°$ is shown in Fig. 1. Limited angular distributions of states observed at 4.97 (2^-) and 5.63 (3^-) MeV and an unresolved multiplet of states at ~7.1 ($3^- + 0^+ + 4^-$) MeV excitation are shown in Fig. 2. Statistical, background subtraction, and peak separation errors are shown.

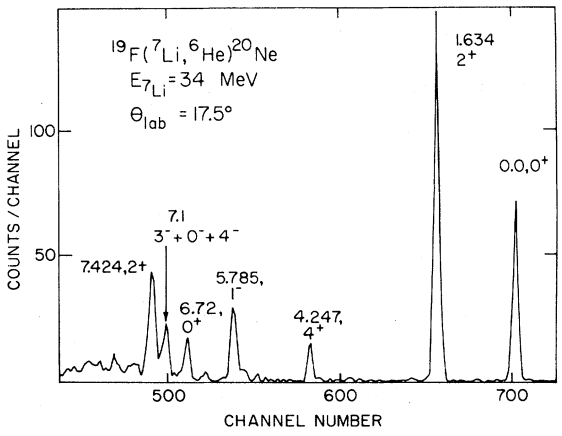

FIG. 1. ^{19}F(^{7}Li, ^{6}He)^{20}Ne spectrum at $\theta_{\mathrm{lab}} = 17.5°$.

IV. ANALYSIS

A. Optical model analysis

The angular distributions for elastic scattering of ^{6}Li and ^{7}Li on ^{19}F were fitted assuming an optical model potential of the following form[13]:

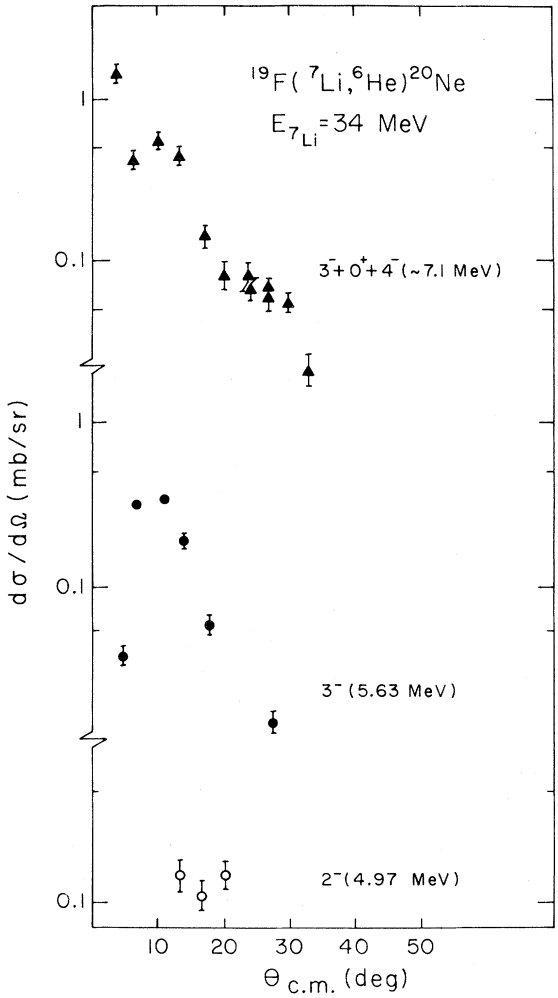

FIG. 2. Angular distributions for transitions to ^{20}Ne states at 4.97 MeV (2^-) and 5.63 MeV (3^-) and for an unresolved multiplet of states at ~7.1 MeV ($3^- + 0^+ + 4^-$).

TABLE I. Optical model parameters.

	E_{lab} (MeV)	U (MeV)	r_R [a] (fm)	a_R (fm)	WS (MeV)	r_I [a] (fm)	a_I (fm)	$4WD$ (MeV)	r_I' [a] (fm)	a_I' (fm)	r_c [a] (fm)
Set 1											
^{7}Li + ^{19}F	34.0	198.49	1.235	0.733	26.01	2.01	0.71	···	···	···	2.0
^{6}Li + ^{19}F	34.0	164.79	1.22	0.733	20.86	2.06	0.69	···	···	···	2.05
Set 2											
^{7}Li + ^{19}F	34.0	198.49	1.235	0.733	13.11	2.01	0.10	39.85	2.01	0.60	2.0
^{6}Li + ^{19}F	34.0	164.79	1.22	0.733	20.86	2.06	0.10	29.22	2.06	0.59	2.05
Set 3 [b]											
^{7}Li + ^{16}O	36.0	189.5	1.21	0.743	21.3	2.0	0.821	···	···	···	2.0
^{6}Li + ^{16}O	36.0	164.3	1.21	0.826	10.6	2.017	1.064	···	···	···	2.1
Set 4 [c]											
^{7}Li + ^{24}Mg	34.0	195.32	1.21	0.78	31.23	1.67	0.89	···	···	···	2.0
^{6}Li + ^{24}Mg	34.0	161.9	1.21	0.80	17.3	1.85	0.89	···	···	···	2.1

[a] $R_x = r_x A_T^{1/3}$.
[b] Reference 15.
[c] Reference 16.

$$V(r) = \frac{-U}{1+\exp[(r-R_R)/a_R]} - \frac{iWS}{1+\exp[(r-R_I)/a_I]} - \frac{4iWD\exp[(r-R_I')/a_I']}{\{1+\exp[(r-R_I')/a_I']\}^2} + V_c, \quad (1)$$

where

$$V_c = \begin{cases} \dfrac{Z_P Z_T e^2}{2R_c}[3-(r/R_c)^2], & r \le R_c \\ \dfrac{Z_P Z_T e^2}{r}, & r > R_c \end{cases}$$

and $R_x = r_x A_T^{1/3}$, A_T is the mass of the target, and Z_P and Z_T are the charges of the projectile and target, respectively. Best fits to the data were obtained using only an imaginary volume absorptive potential ($WD = 0$). The computer code[14] JIB was used to perform these fits. The results are listed as optical model parameter Set 1 in Table I. These parameters are very similar to those obtained by Schumacher *et al.*[15] to fit elastic scattering of 36 MeV ^{6}Li and ^{7}Li from ^{16}O. The Schumacher *et al.* parameters are listed in Table I as optical parameter Set 3. Parameters obtained[16] for ^{6}Li and ^{7}Li scattering on ^{24}Mg are listed as Set 4. The fit to the data using Set 1 is shown in Fig. 3 for ^{7}Li + ^{19}F and ^{6}Li + ^{19}F. The sharp rise of the cross section with decreasing angle could not be reproduced well by the optical model, but the structure in the angular distribution at larger angles is reasonably well reproduced. The normalization of the forward angle points was checked, but no systematic error could be found. A similar result was observed for Li scattering by ^{24}Mg.

Baltz, Bond, Garrett, and Kahana[17] have proposed a phenomenological imaginary potential consisting of a deep volume term (WS) of small diffusivity (a_I) and a shallow surface term (WD) with standard diffusivity (a_I') and have used it in DWBA calculations to reproduce the shapes of angular distributions for such reactions as ^{40}Ca(^{13}C, ^{12}C)^{41}Ca$_{g.s.}$, ^{40}Ca(^{13}C, ^{14}N)^{39}K$_{g.s.}$, and ^{60}Ni(^{18}O, ^{16}O)^{62}Ni. They argue that as the separation between the centers of projectile and target decreases, compound reactions begin to take place which sharply decrease the "... probability for exit into direct channels. The onset of such processes as a function of the (decreasing) separation between centers is likely to be sudden." The volume part of the potential, with small diffusivity, simulates the rapid surface change. Because Baltz *et al.* had reasonable success reproducing the magnitude and the phase of the ^{40}Ca(^{13}C, ^{14}N)^{39}K$_{g.s.}$ angular distribution, we have investigated an optical model potential of the same form for ^{6}Li and ^{7}Li scattering on ^{19}F to use in the subsequent DWBA analyses. The computer code[13] OPTIX1 was used to fit the elastic scattering data. A diffusivity of 0.10 fm was used for the volume imaginary potential. The surface and volume imaginary potential depths and the surface imaginary diffusivities were varied to yield the best fits of the optical model angular distributions to the data. The best fit parameters for this form of the optical model potential are listed as Set 2 in Table I. The fits for ^{7}Li and ^{6}Li elastic scattering on ^{19}F are shown in Fig. 3. The calculations using optical parameter Sets 1 and 2 differ in phase at angles $\theta_{c.m.} > 50°$ and the calculations using Set 1 give a slightly better fit to the data.

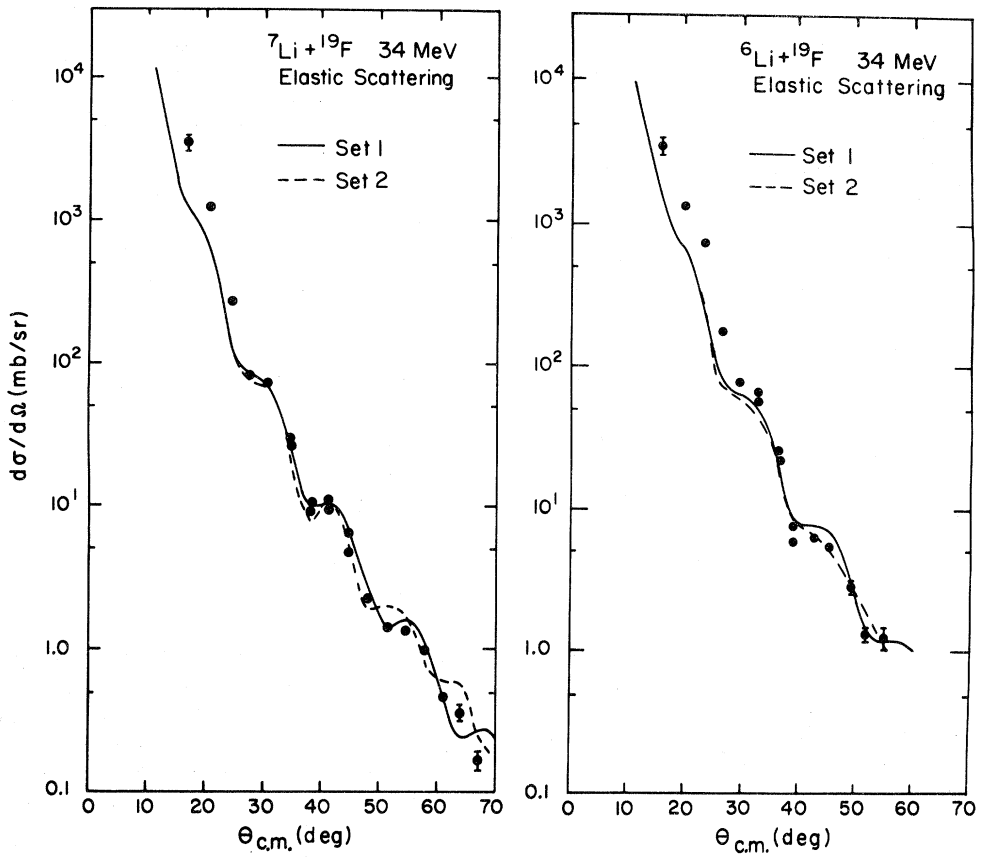

FIG. 3. Cross sections and optical model calculations for elastic scattering of 34 MeV ^{6}Li and ^{7}Li from ^{19}F. The solid line is fitted using optical parameter Set 1; dashed line, parameter Set 2.

B. DWBA analysis

Exact finite range DWBA calculations using the code MERCURY[18] were performed with the optical model parameter Sets 1, 2, 3, and 4 (Table I) for some or all of the ^{19}F(^{7}Li, ^{6}He)^{20}Ne transitions. The ^{6}Li parameters were used for the ^{6}He exit channel in all cases.[1,2] Experimental angular distributions and DWBA fits, based on calculations using optical parameter Set 1, for transitions to the 0^+ (0.0 MeV), 2^+ (1.634 MeV), 4^+ (4.247 MeV), 1^- (5.785 MeV), 0^+ (6.722 MeV), and 2^+ (7.424 MeV) states in ^{20}Ne are shown in Fig. 4. A radius $r_0 = 1.25$ fm and diffusivity $a = 0.65$ fm were used in the calculations of the bound state wave functions for protons in $2s_{1/2}$, $2p_{1/2}$, $2p_{3/2}$, $1d_{3/2}$, $1d_{5/2}$, $1g_{7/2}$, or $1g_{9/2}$ orbits in ^{20}Ne and for the $1p_{3/2}$ proton in ^{7}Li. The bound state potential well depths were determined by varying the depths until the proper binding energies were achieved.

For the transitions to the 0^+ states at 0.0 and 6.722 MeV, a single orbital angular momentum transfer, $l = 1$, is allowed. In both cases, the slopes of the experimental and calculated angular distributions are about the same, but the oscillations in the calculation are out of phase with the data over most of the angular range. A similar effect has been noted for $2s_{1/2}$ transitions[16] in ^{24}Mg(^{7}Li, ^{6}Li)^{25}Mg. Calculations using the surface transparent optical parameters, Set 2, are out of phase with the data by the same amount as those of parameter Set 1. Although one might expect some shift in phase with the surface transparent form of the optical model potential because contributions from the nuclear interior would be different,[17] no change is observed in this calculation. The agreement in both phase and magnitude for the calculations using parameter Sets 1 and 2 can be understood by comparing the shapes of the imaginary potentials, as shown in Fig. 5. The potentials are the same in the region of the "critical radius" where much of the absorption occurs[19] and, therefore, where direct reactions would be expected to occur.

Angular momentum selection rules[16] allow three possible l transfers, $l = 1$, 2, or 3, when a 2^+ state in ^{20}Ne is populated by transfer of a proton into a $d_{3/2}$ or $d_{5/2}$ single particle state. Each $d_{3/2}$

or $d_{5/2}$ transfer cross section is composed of an incoherent sum of $l = 1$, 2, and 3 transfer cross sections. The angular distribution for the transition to the 2^+ state at 1.634 MeV was fitted by an incoherent sum of $d_{3/2}$ and $d_{5/2}$ cross sections, but the angular distribution for the 7.424 MeV state was best fitted by only a $d_{3/2}$ cross section. The angular distribution for the transition to the 1^- state at 5.785 MeV was fitted by an incoherent sum of $2p_{1/2}$ and $2p_{3/2}$ transfer cross sections.

For the j-forbidden transition to the 4^+ state, the most important difference observed between the (^{3}He, d) and (^{7}Li, ^{6}He) reactions is the shape of the angular distributions. For the same energy above the Coulomb barrier, the (^{3}He, d) angular distribution[3] is constant between 20° and 60° c.m., while the (^{7}Li, ^{6}He) reaction decreases in cross section by a factor of 10. Since the shape of the 4^+ (^{7}Li, ^{6}He) angular distribution is characteristic of a single step stripping reaction, DWBA calculations were done assuming the transferred proton to enter either a $1g_{9/2}$ or $1g_{7/2}$ orbit in ^{20}Ne. A bound state well depth of 135 MeV was required to bind the g state protons when the bound stage geometrical parameters were $r_0 = 1.25$ fm and $a = 0.65$ fm. The best fit to the 4^+ data was obtained for a pure $g_{9/2}$ transfer. The results of the calculations are shown in Fig. 4.

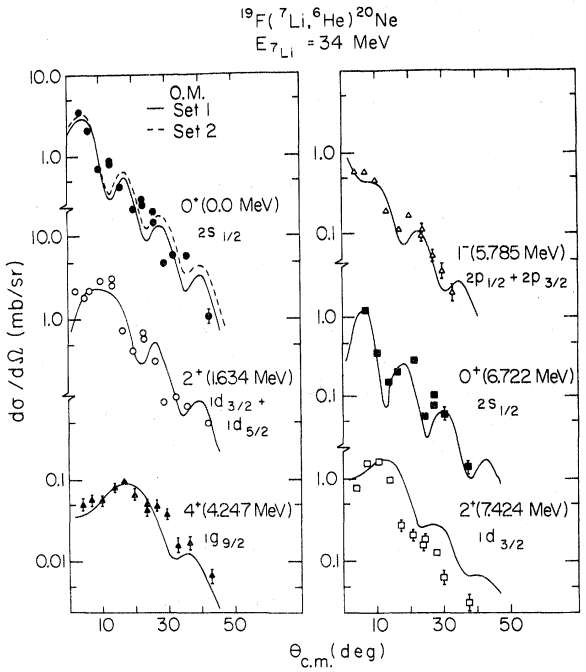

FIG. 4. Angular distributions and finite-range DWBA calculations for transitions to ^{20}Ne states at 0.0 MeV (0^+, $2s_{1/2}$ transfer), 1.634 MeV (2^+, $1d_{3/2} + 1d_{5/2}$ transfer), 4.247 MeV (4^+, $1g_{9/2}$ transfer), 5.785 MeV (1^-, $2p_{1/2} + 2p_{3/2}$ transfer), 6.722 MeV (0^+, $2s_{1/2}$ transfer), and 7.424 MeV (2^+, $1d_{3/2}$ transfer). Solid lines are calculations done with optical model parameter Set 1, while the dashed line is a calculation with Set 2.

C. Spectroscopic factors

The differential cross sections calculated by the DWBA code MERCURY,[17] $\sigma_j(\theta)$, are related to the experimental cross sections by the following equation:

$$\sigma_{\exp}(\theta) = \sum_j C^2S_{1j}(\exp) C^2S_2 \sigma_j(\theta), \tag{2}$$

where C^2S_2, the spectroscopic factor which describes the overlap of ^{7}Li with ^{6}He $+p$, is taken from Cohen and Kurath[20] to be 0.59 and C^2S_{1j} (exp) is the spectroscopic factor for total angular momentum transfer j determined from fitting the data with an incoherent sum of calculated cross sections. The spectroscopic factors extracted by fitting the data with cross sections calculated using optical model parameter Sets 1, 2, 3, and 4 are listed in Table II. The spectroscopic factors extracted from fits to the 34 MeV data for calculations using parameter Set 1 (the parameters determined from fitting ^{6}Li and ^{7}Li scattering on ^{19}F) and parameter[15] Set 3 agree within approximately 10%. Those extracted using Set 4 are 35% smaller. The spectroscopic factors obtained for the transition to the 0.0 MeV (0^+) state using standard optical model parameter Set 1, and the surface transparent potential, Set 2, agree to within about 15%.

The spectroscopic factors extracted for the 4^+ state from data taken at 34 MeV (over an angular range of 3° to 40° in the lab) and at 37 MeV (over a limited range from 10° to 20°—the region where

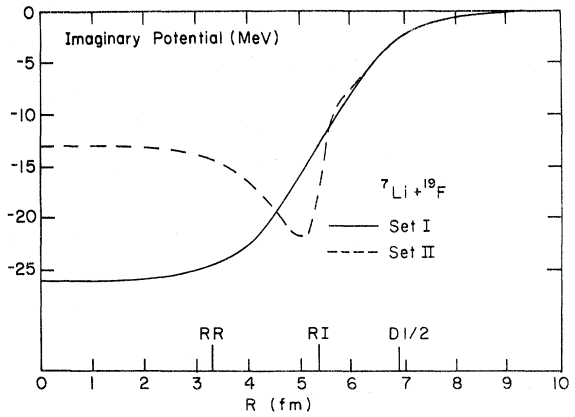

FIG. 5. Imaginary potentials as a function of radius for optical parameter Set 1 (solid line) and Set 2 (dashed line). $D_{1/2}$ is the "critical radius" (Ref. 19).

TABLE II. Spectroscopic factors $C^2S_{l_j}$(exp).

E_x (MeV)	l_j	Set 1 (34 MeV)	Set 2 (34 MeV)	Set 3 (34 MeV)	Set 3 (37 MeV)	Set 4 (34 MeV)	C^2S (model)
0.0	$s_{1/2}$	0.364	0.312	0.369	0.647	0.275	0.502
1.634	$d_{3/2}$	0.237	···	0.229	···	···	0.224
	$d_{5/2}$	0.304	···	0.324	···	···	0.087
	sum	0.541	···	0.553	0.671	0.362	0.311
4.247	$g_{7/2}$	0.0	···	0.0	···	···	0.003
	$g_{9/2}$	0.066	···	0.06	···	···	0.003
	sum	0.066	···	0.06	0.06	···	0.006
5.785	$p_{1/2}$	0.008	···	0.008	···	···	0.023
	$p_{3/2}$	0.026	···	0.024	···	···	0.138
	sum	0.034	···	0.032	···	···	0.261
6.722	$s_{1/2}$	0.202	···	0.174	···	···	0.251
7.424	$d_{3/2}$	0.222	···	0.198	···	···	0.099
	$d_{5/2}$	0.0	···	0.003	···	···	0.044
	sum	0.222	···	0.201	···	···	0.143

the cross section peaks) agree very well. The agreement for the 2^+ and 0^+ states is not as good. This poorer agreement is probably because the cross sections vary rapidly in the region from 10° to 20° in the lab and the fit to the data is very sensitive to differences in the phases of the calculated and experimental angular distributions.

Listed in Table II are spectroscopic factors calculated using the Nilsson model. Nilsson coefficients C_{nlj} were calculated with the code NEPTUNE[21] assuming a deformation[22] β of 0.45. The Nilsson model spectroscopic factor is given by

$$C^2S(\text{model}) = \frac{2}{2J_F+1} C_{nlj}^{\ 2} \tag{3}$$

for members of the ground state rotational band, and for all other states

$$C^2S(\text{model}) = \frac{1}{2J_F+1} C_{nlj}^{\ 2}, \tag{4}$$

where J_F is the angular momentum of the final state. The agreement between predicted and extracted spectroscopic factors is reasonably good, considering the simplicity of the model, except for the 4^+ state, which is about a factor of ten stronger than predicted and for the 1^- state, about eight times weaker than predicted.

Table III lists spectroscopic factors extracted in the present work, extracted in other experiments,[3-5] and predicted by the Nilsson and shell models.[23] Agreement between the (^{7}Li, ^{6}He) spectroscopic factors and those obtained in light-ion transfer reactions is good. One notes that the spectroscopic factor for the 2^+ state at 7.424 MeV is 30–50% larger than observed in other reactions. The 4^+ state was observed to be strongly excited in the (^{3}He, *d*) reaction.[3,4] Obst and Kemper[3] attribute this strong excitation to multistep processes and thus do not report a spectroscopic factor for this state. The Nilsson model appears to overestimate the 0^+ (0.0 MeV) spectroscopic factor and the shell model predicts both 0^+ spectroscopic

TABLE III. Comparison of spectroscopic factors (C^2S).

^{20}Ne E_x (MeV)	J^π	(^{7}Li, ^{6}He) (34 MeV)	(^{3}He, *d*)[a] (20–23 MeV) DWBA	(^{3}He, *d*)[a] (20–23 MeV) CCBA	(^{3}He, *d*)[b] (10 MeV)	(*d*, *n*)[c] (3 MeV)	Nilsson model	Shell model[d]
0.0	0^+	0.36	0.30	0.43	0.31	0.62	0.502	0.72
1.634	2^+	0.54	0.42	0.38	0.62	0.70	0.311	0.43
4.247	4^+	0.06	0.00	0.00	≤0.21	···	0.006	0.0
5.785	1^-	0.03	0.04	0.04	0.05	···	0.261	0.006
6.722	0^+	0.20	0.25	0.22	0.47	0.38	0.251	0.48
7.424	2^+	0.22	0.12	0.12	0.16	···	0.143	0.11

[a] Reference 3.
[b] Reference 4.
[c] Reference 5.
[d] Reference 23.

factors to be larger than observed. The 1^- spectroscopic factor is predicted to be too large by the Nilsson model and too small (by a factor of about 7) by the shell model.

V. CONCLUSIONS

Spectroscopic factors extracted from ^{19}F-(^{7}Li, ^{6}He)^{20}Ne are in good agreement with those determined by light-ion transfer reactions. This indicates again that (^{7}Li, ^{6}He) is useful for obtaining spectroscopic information.

The slope as well as the width and depth of oscillations of the single nucleon transfer cross sections are well reproduced by the DWBA calculations. There is a severe phase problem: oscillations peak farther forward for the data than predicted by the calculations so that experimental and DWBA cross sections are out of phase. Changing optical parameters or even making use of an optical model potential with a volume term with small diffusivity plus a surface term does not appear to improve the phase agreement. This phase discrepancy seems to be especially severe for light targets (Be, F, Mg, etc.) and has been also reported for the ^{12}C(^{14}N, ^{13}N)^{13}C reaction.[24] The trouble may be with the calculation of the form factor and may indicate that theoretical work needs to be done for strongly deformed nuclei.

The weak excitation of the 4^+ state in ^{20}Ne via the ^{19}F(^{7}Li, ^{6}He)^{20}Ne reaction seems to indicate that multistep processes are less important for the population of this state in this reaction than in (^{3}He, d) and in the ^{19}F(^{16}O, ^{15}N)^{20}Ne reactions[25] for similar energies above the Coulomb barrier in the three reactions. Finite-range coupled channel Born-approximation (CCBA) calculations[26] by Nagel and Koshel which include inelastic coupling in both the entrance and exit channels could explain neither the strength of population of j-forbidden states in ^{25}Mg or ^{25}Al nor the phase problem. Because the first maximum in the 4^+ cross section is reasonably well fit with DWBA calculation, it is probable that a large part of the transfer cross section is due to direct $g_{9/2}$ transfer. Proton stripping reactions on ^{19}F are a convenient way to study multistep transitions in heavy-ion reactions, since the poor energy resolution which normally occurs does not prevent the j-forbidden transition from being extracted. While the ^{19}F(^{16}O, ^{15}N) reaction[25] has been measured, no DWBA calculations were reported, so that a comparison with the present results was not possible. Clearly, measurements of the reactions ^{19}F(^{14}N, ^{13}C), ^{19}F(^{15}N, ^{14}C), ^{19}F(^{12}C, ^{11}B) with full finite range CCBA analyses of the data are needed before any conclusions about multistep processes in heavy-ion reactions can be made.

---

†Work supported in part by the National Science Foundation under Grants Nos. NSF-MPS-750-3767, NSF-GJ-367, and NSF-GU-2612.

*Present address: Physics Department, Ripon College, Ripon, Wisconsin 54971.

‡Present address: Physics Department, University of Pennsylvania, Philadelphia, Pennsylvania 19174.

§Present address: National Electrostatics Corporation, Middleton, Wisconsin 53562.

‖Present address: Department of Nuclear Physics, The Australian National University, Box 4, P. O. Canberra, A.C.T. Australia 2600.

[1]R. L. White, K. W. Kemper, L. A. Charlton, and G. D. Gunn. Phys. Rev. Lett. 32, 892 (1974).

[2]R. L. White and K. W. Kemper, Phys. Rev. C 10, 1372 (1974).

[3]A. W. Obst and K. W. Kemper, Phys. Rev. C 8, 1682 (1973).

[4]R. H. Siemssen, L. L. Lee, Jr., and D. Cline, Phys. Rev. 140, B1258 (1965).

[5]R. H. Siemssen, R. Felst, M. Cosack, and J. L. Weil, Nucl. Phys. 52, 273 (1964).

[6]M. C. Mermaz, C. A. Whitten, Jr., and D. A. Bromley, Phys. Rev. 187, 1466 (1969).

[7]M. E. Williams, G. M. Hudson, K. W. Kemper, G. E. Moore, G. A. Norton, R. J. Puigh, and L. A. Charlton, Bull. Am. Phys. Soc. 19, 993 (1974).

[8]E. Heinicke and H. Baumann, Nucl. Instrum. Methods 58, 125 (1968).

[9]R. Middleton and C. T. Adams, Nucl. Instrum. Methods 118, 329 (1974).

[10]K. R. Chapman, Nucl. Instrum. Methods 124, 299 (1975).

[11]G. R. Morgan, G. D. Gunn, M. B. Greenfield, N. R. Fletcher, J. D. Fox, D. McShan, and L. Wright, Nucl. Instrum. Methods 123, 439 (1975).

[12]K. Bethge, C. M. Fou, R. W. Zurmühle, Nucl. Phys. A123, 521 (1969).

[13]W. J. Thompson and E. Gille, Florida State University Technical Report No. 9, 1966 (unpublished).

[14]F. G. Perey, Phys. Rev. 131, 745 (1963); A. W. Obst, Florida State University Technical Report JIB (unpublished).

[15]P. Schumacher, N. Ueta, H. H. Duhm, K.-I. Kubo, and W. J. Klages, Nucl. Phys. A212, 573 (1973).

[16]G. E. Moore, K. W. Kemper, and L. A. Charlton, Phys. Rev. C 11, 1099 (1975).

[17]A. J. Baltz, P. D. Bond, J. D. Garrett, and S. Kahana, Phys. Rev. C (to be published).

[18]L. A. Charlton, Phys. Rev. C 8, 146 (1973); L. A. Charlton and D. Robson, Florida State University Technical Report No. 5, MERCURY (unpublished).

[19]G. R. Satchler, in *Proceedings of the International Conference on Reactions between Complex Nuclei, Nashville, Tennessee, 1974,* edited by R. L. Robinson and J. H. Hamilton (North-Holland, Amsterdam/Amer-

ican Elsevier, New York, 1974), Vol. 2, p. 171.
[20]S. Cohen and D. Kurath, Nucl. Phys. A101, 1 (1967).
[21]T. Tamura, University of Texas Report, NEPTUNE, 1971 (unpublished).
[22]K. W. Kemper, D. S. Haynes, and N. R. Fletcher, Phys. Rev. C 4, 108 (1971).
[23]J. B. McGrory and B. H. Wildenthal, Phys. Rev. C 7, 974 (1973).
[24]R. M. DeVries, M. S. Zisman, J. G. Cramer, K. L. Liu, F. D. Becchetti, B. G. Harvey, H. Homeyer, D. G. Kovar, J. Mahoney, and W. von Oertzen, Phys. Rev. Lett. 32, 680 (1974).
[25]F. Pougheon, G. Rotbard, P. Roussel, and J. Vernotte, Phys. Rev. Lett. 34, 158 (1975).
[26]P. Nagel and R. D. Koshel, Bull. Am. Phys. Soc. 20, 716 (1975).